

# Synthesis, spectroscopic, thermal, voltammetric studies and biological activity of crystalline complexes of pyridine-2,6-dicarboxylic acid and 8-hydroxyquinoline

Alper Tolga Çolak<sup>a,\*</sup>, Ferdağ Çolak<sup>b</sup>, Okan Zafer Yeşilel<sup>c</sup>, Orhan Büyükgüngör<sup>d</sup>

<sup>a</sup> Department of Chemistry, Faculty of Arts and Sciences, Dumlupınar University, 43820 Kütahya, Turkey

<sup>b</sup> Department of Biology, Faculty of Arts and Sciences, Dumlupınar University, 43820 Kütahya, Turkey

<sup>c</sup> Department of Chemistry, Faculty of Arts and Sciences, Eskişehir Osmangazi University, 26480 Eskişehir, Turkey

<sup>d</sup> Department of Physics, Faculty of Arts and Sciences, Ondokuz Mayıs University, 55139 Kurupelit, Samsun, Turkey

## ARTICLE INFO

### Article history:

Received 13 February 2009

Received in revised form 29 May 2009

Accepted 21 July 2009

Available online 25 July 2009

### Keywords:

Dipicolinate complexes

8-Hydroxyquinoline

Antimicrobial activity

Cyclic voltammograms

## ABSTRACT

Two new compounds (8-H<sub>2</sub>Q)<sub>2</sub>[M(dipic)<sub>2</sub>].6H<sub>2</sub>O (M = Co (**1**) and Ni (**2**), 8-HQ = 8-hydroxyquinoline, dipic = dipicolinate) have been prepared and characterized by elemental analysis, spectral (IR and UV–vis), thermal analyses, magnetic measurements and single-crystal X-ray diffraction techniques. Both **1** and **2** consist two 8-hydroxyquinolinium cations, one bis(dipicolinate)M(II) anion [M = Co(II), Ni(II)] and six uncoordinated water molecules. Both **1** and **2** crystallize in the monoclinic space group C2/c. In the compounds anion, each dipic ligand simultaneously exhibits tridentate coordination modes through N atom of pyridine ring and oxygen atoms of the carboxylate groups. The crystal packing of **1** and **2** is a composite of intermolecular hydrogen bonding and C–O...π interactions. The *in vitro* antibacterial and antifungal activities of **1** and **2** were evaluated by the agar well diffusion method by MIC tests. Both new compounds showed the same antimicrobial activity against Gram-positive bacteria and yeast and fungi except Gram-negative bacteria.

© 2009 Elsevier B.V. All rights reserved.

## 1. Introduction

Pyridine-2,6-dicarboxylic acid (dipicolinic acid, H<sub>2</sub>dipic) was first discovered in a biological system in 1936 and is now known to be a major component of bacterial spores [1]. H<sub>2</sub>dipic is used in a variety of processes as an enzyme inhibitor, plant preservative and food sanitizer [2]. Recent investigations of the H<sub>2</sub>dipic exhibit that this acid prevents the oxidation of low density lipoprotein, the substance, whose oxidation is involved in the pathogenesis of arteriosclerosis [3]. H<sub>2</sub>dipic is a polar aromatic acid that is soluble in organic and chlorinated solvents in the acidic form and thus can penetrate lipid interfaces and be solubilized in hydrophobic environments [4]. H<sub>2</sub>dipic has been studied extensively as a Lewis base. H<sub>2</sub>dipic and its anions (Hdipic<sup>−</sup>, dipic<sup>2−</sup>) have proved to be well suited for the construction of multidimensional frameworks, due to the presence of two adjacent O atoms of carboxylate groups as substituents on the N-heterocyclic pyridine ring [2,5]. Among the diversity of pyridine-2,6-dicarboxylic acid complexes known, potential applications, in fields of aqueous chemistry, catalysis, biochemistry, as water-soluble drugs, antitumor activity, magnetic materials, in bleaching, bactericidal compositions, development

of more effective anti-HIV agents and the design of insulin-mimetic agents [2,5–8]. Previous studies have shown that a series of vanadium-dipicolinate complexes is effective on diabetic hyperglycemia and vanadium(V) can have insulin mimetic properties when the organic ligand has been chosen appropriately [9–11]. The [Co(dipic)<sub>2</sub>]<sup>2−</sup> was found to be effective in reducing the hyperlipidemia of diabetes using oral administration in drinking water in rats with streptozotocin-induced diabetes [12]. Mixed ligand complexes have a key role in biological chemistry because the mixed chelation occurs commonly in biological fluids as millions of potential ligands are likely to compete for metal ions *in vivo* [13]. Although a high number of pyridine-2,6-dicarboxylic acid complexes of almost all transition metals is known, studies of biologic [13–17] and electrochemical [18,19] activity with the complexes of this ligand are rather scant and appear to be limited to only a few examples based on transition metals. Single-crystal X-ray structure determinations of other Co(II)–dipic, Ni(II)–dipic, Cu(II)–dipic proton transfer compounds are (HIm)<sub>2</sub>[Co(dipic)<sub>2</sub>].2H<sub>2</sub>O [20], (HIm)<sub>2</sub>[Ni(dipic)<sub>2</sub>].2H<sub>2</sub>O [20], (H<sub>2</sub>pipz)[Ni(dipic)<sub>2</sub>].4H<sub>2</sub>O [21], (HQx)<sub>2</sub>[Cu(Hdipic)<sub>2</sub>].6H<sub>2</sub>O [22] (Im = imidazole, pipz = piperazine, HOx = 8-hydroxyquinoline).

The treatment of infectious diseases still remains an important and challenging problem because of a combination of factors including emerging infectious diseases and the increasing number of multi-drug resistant microbial pathogens [23]. Decreased

\* Corresponding author.

E-mail address: [acolak@dumlupinar.edu.tr](mailto:acolak@dumlupinar.edu.tr) (A.T. Çolak).

efficacy and resistance of pathogens to compounds has necessitated development of new alternatives. In light of these problems, the search for new antimicrobial agents has gained immense popularity in the field of drug development.

In this study, we describe the preparation, spectroscopic, thermal, structural characterization, antimicrobial activities and electrochemical studies of  $H_2dipic$  complexes of cobalt(II) and nickel(II) with 8-hydroxyquinoline,  $(8-H_2Q)_2[Co(dipic)_2] \cdot 6H_2O$  (**1**)  $(8-H_2Q)_2[Ni(dipic)_2] \cdot 6H_2O$  (**2**).

## 2. Experimental

### 2.1. Materials and equipment

All chemicals and solvents used for the synthesis were of reagent grade. Pyridine-2,6-dicarboxylic acid, 8-hydroxyquinoline,  $Co(CH_3COO)_2 \cdot 4H_2O$ ,  $Ni(CH_3COO)_2 \cdot 4H_2O$  and  $C_2H_5OH$  (Aldrich) were used as received. Elemental analyses (C, H, and N) were performed using a Vario EL III CHNS elemental analyzer. Magnetic susceptibility measurements were performed at room temperature using a Sherwood Scientific MK1 model Gouy magnetic balance. UV-vis spectra were obtained in the methanol solutions ( $10^{-3}$  mol/L) of the complex with a Shimadzu Pharmaspec UV-1700 spectrometer in the range of 1000–190 nm. FT-IR spectra were recorded in the  $4000\text{--}400\text{ cm}^{-1}$  region with a Bruker Optics, Vertex 70 FT-IR spectrometer using KBr pellets. Diamond TG/DTA thermal analyzer was used to record simultaneous TG, DTG and DTA curves in nitrogen **1** and **2** in static air atmosphere at a heating rate of  $10\text{ K min}^{-1}$  in the temperature range  $35\text{--}1000\text{ }^\circ\text{C}$  using platinum crucibles.

### 2.2. X-ray crystallography

Data collection (**1**) and (**2**) were performed on a STOE IPDS II image plate detector using  $MoK_\alpha$  radiation ( $\lambda = 0.71019\text{ \AA}$ ). Intensity data were collected in the  $\theta$  range  $2\text{--}25.5^\circ$  at  $293(2)\text{ K}$ . Data collections: Stoe X-Area [24]. Cell refinement: Stoe X-Area [24]. Data reduction: Stoe X-RED [24]. The structure was solved by direct methods and anisotropic displacement parameters were applied to non-hydrogen atoms in a full-matrix least-squares refinement based on  $F^2$  using SHELXL-97 [25]. Molecular drawings were obtained using ORTEP-III [26].

### 2.3. Biological activity of compounds

Microbial strains; A total of 6 microbial species including 4 bacteria, 1 molds and 1 yeast were used as test organisms in this study. *Staphylococcus aureus* ATCC 25923, *Escherichia coli* ATCC 25922 *Salmonella typhimurium* ATCC 14028, *Aspergillus niger* ATCC 10949, *Candida albicans* (ATCC 10231) were obtained from American Type Culture Collection; *Bacillus subtilis* NRRL-B-209 from USDA, Agriculture Research Service, Peria, USA. Bacterial and fungal cultures of test organisms were maintained on Nutrient Agar and Malt Extract Agar slants at  $4\text{ }^\circ\text{C}$ , respectively, and were subcultured in petri dishes prior to use. Antimicrobial activity analysis of test compounds was carried out according to modified agar well diffusion assay [27,28]. The following test conditions were applied; compound was dissolved in Dimethylsulfoxide (DMSO, Merck). Fifteen milliliters of the specified molten agar ( $45\text{ }^\circ\text{C}$ ) were poured into sterile Petri dishes ( $\varnothing 90\text{ mm}$ ). The cell suspensions containing  $10^8$  CFU/mL cells for bacteria,  $10^7$  CFU/mL cells for yeasts, and  $10^5$  spore/mL of fungi were prepared and evenly spread onto the surface of the agar plates of Nutrient Agar (Fluka) for bacteria and yeast and Potato Dextrose Agar (Merck) medium for fungi using sterile swab sticks. The plates were dried aseptically at

$35\text{ }^\circ\text{C}$  for about 40 min in an incubator. The agar well method for the estimation of MIC values (the lowest concentration of compounds required to inhibit the growth of the tested microorganisms) was applied to evaluate the antimicrobial activity. At the same time, 10 mm wells were bored using a sterile cork borer and impregnated with known concentrations which were previously determined by MIC tests ( $250\text{--}0.4\text{ }\mu\text{g/mL}$  for each well) from each compound ( $100\text{ }\mu\text{L}$ ) and the synthesized compounds **1** and **2** were placed into the wells. The plates were preincubated for 2 h at room then the plates were incubated at  $37\text{ }^\circ\text{C}$  for 24 h for bacterial strains, 48 h for yeasts and 72 h for fungi at room temperature. Tetracycline ( $30\text{ }\mu\text{g/mL}$ ) for bacteria was used as positive control. DMSO was used as negative control. Antimicrobial activity was evaluated as zones of inhibition of growth around wells. All samples were tested in triplicate.

### 2.4. Synthesis of $(8-H_2Q)_2[Co(dipic)_2] \cdot 6H_2O$ (**1**) and $(8-H_2Q)_2[Ni(dipic)_2] \cdot 6H_2O$ (**2**)

A solution of  $[Co(H_2dipic)(dipic)] \cdot 3H_2O$  [12] or  $[Ni(Hdi-dipic)_2] \cdot 3H_2O$  [29] (1 mmol, 0.445 g) in ethanol–water (1:1; 40 mL) was added drop wise by stirring at room temperature to a solution of 8-hydroxyquinoline (2 mmol, 0.290 g). After 60 min stirring at room temperature, resulting clear red (**1**) and green (**2**) solutions were observed. After one week, formed crystals were filtered and washed with 20 mL of cold ethanol and dried on air. Yields 0.52 g (66%) and 0.48 g (61%). *Anal. calcd.* for (**1**)  $C_{32}H_{34}N_4O_{16}Co$  : C, 48.7; H, 4.3; N, 7.1. Found: C, 48.6; H, 4.4; N, 7.2%. *Anal. calcd.* for (**2**)  $C_{32}H_{34}N_4O_{16}Ni$  : C, 48.7; H, 4.3; N, 7.1. Found: C, 48.7; H, 4.3; N, 7.1%.

## 3. Results and discussion

### 3.1. UV-vis spectra and magnetic susceptibilities

Electronic absorption spectrum of **1** displays the visible asymmetric region maximum at  $\lambda_{max} = 556\text{ nm}$  ( ${}^4T_{1g} \rightarrow {}^4A_{2g}$  transition). The electronic spectrum of **2** in  $H_2O$  exhibits three absorption bands at 371, 508, 617 nm and the corresponding  $\epsilon$  values are 43, 32,  $35\text{ L mol}^{-1}\text{ cm}^{-1}$ . These values were assigned to the following  $d\text{--}d$  transitions;  ${}^3A_{2g} \rightarrow {}^3T_{1g}$  (P),  ${}^3A_{2g} \rightarrow {}^3T_{1g}$  and  ${}^3A_{2g} \rightarrow {}^3T_{2g}$ , respectively. The  $\Delta_o$  value for **2** was calculated as  $10941\text{ cm}^{-1}$ , since  $\Delta_o = \nu_1$  for  $d^8$  complexes.

The complex **1** shows room temperature magnetic moments in the range of 5.21 BM corresponding to three unpaired electrons which suggest an octahedral geometry. This value is higher than the spin-only value of 3.87. Because, not only the spin magnetic moment contribute to the total magnetic moment but also orbital magnetic moment in Co(II) complexes. For orbital angular momentum to contribute, and hence for the paramagnetism to differ significantly from the spin-only value, there must be an unfilled or half-filled orbital similar in energy to that of the orbitals occupied by the unpaired spins. If that is so, the electrons can make use of the available orbital to circulate around the center of the complex and hence generate angular momentum and a magnetic moment [30]. The complex **2** exhibits magnetic moment value of 2.90 BM, which suggests an octahedral geometry.

### 3.2. FT-IR spectra

The most significant frequencies in the IR spectrum of **1** are given in Table S3. The strong and broad absorption bands at  $3480$  (**1**) and  $3491\text{ cm}^{-1}$  (**2**) are attributed to the  $\nu(OH)$  vibrations of crystal water molecules. The absorption bands at 3370, 3376 and  $3193$ ,  $3191\text{ cm}^{-1}$  are related to  $\nu(NH)$  and  $\nu(OH)$  vibrations of 8-HQ

ligands in the IR spectrum of **1** and **2**. The carboxylate groups exhibited strong bands in the region  $1682\text{--}1582\text{ cm}^{-1}$ . These strong bands were shifted and broadened with respect to free dipicolinic acid. The presence of carboxylate  $\text{COO}^-$  is reflected by IR spectrum in absorption bands of the asymmetric ( $\nu_{\text{as}}$ ) and symmetric ( $\nu_{\text{s}}$ ) stretch vibrations at  $1615\text{--}1472\text{ cm}^{-1}$  and  $1609\text{--}1473\text{ cm}^{-1}$ , respectively, and moreover the differences between the asymmetric and symmetric stretches of the carboxylate groups of the complexes  $\Delta = 143$  and  $136\text{ cm}^{-1}$ , respectively, suggest a monodentate binding of the carboxylate group to the metal ion [31]. The absorption bands at  $1589$  and  $1591\text{ cm}^{-1}$  are due to  $\nu(\text{C}=\text{C})+\nu(\text{C}=\text{N})$  vibration of dipic and 8- $\text{H}_2\text{Q}$  (**1**) and (**2**) ligands. The absorption band at  $620$ ;  $428$ , and  $630$ ;  $442\text{ cm}^{-1}$  are attributed to the M–O and M–N vibrations of the complexes.

### 3.3. Thermal analyses

The TG-DTG and DTA curves of the compounds are shown in Figs. 1 and 2. The endothermic peaks of **1** ( $\text{DTA}_{\text{max}} = 91.30\text{ }^\circ\text{C}$ ) between  $35$  and  $102\text{ }^\circ\text{C}$  correspond to the loss of the 6-mol crystal water molecules (found  $13.80$ , calcd.  $13.67\%$ ). The similar results are found for **2** ( $\text{DTG}_{\text{max}} = 91\text{ }^\circ\text{C}$ ; found  $13.30$ , calcd.  $13.68$ ) between  $35$  and  $120\text{ }^\circ\text{C}$ . The anhydrous compound **1** is thermally stable up to about  $125\text{ }^\circ\text{C}$ . Three-mole decarboxylate of dipic molecules and two  $(8\text{-H}_2\text{Q})^+$  groups are lost in two steps ( $\text{DTA}_{\text{max}} = 164.7\text{ }^\circ\text{C}$ ,  $238.6\text{ }^\circ\text{C}$ ; found  $53.80$ , calcd.  $53.74\%$ ) for **1** between  $102$  and  $358\text{ }^\circ\text{C}$ . One-mole decarboxylate of dipic molecules and two  $(8\text{-H}_2\text{Q})^+$  groups are lost in three steps ( $\text{DTG}_{\text{max}} = 180.3\text{ }^\circ\text{C}$ ,  $255.2\text{ }^\circ\text{C}$ ,  $278.1\text{ }^\circ\text{C}$ ; found  $43.60$ , calcd.  $42.61\%$ ) for **2**. The exothermic peaks of **1** ( $\text{DTA}_{\text{max}} = 430.4\text{ }^\circ\text{C}$ ) between  $358$  and  $480\text{ }^\circ\text{C}$  correspond to the loss of the one-mole decarboxylate of dipic molecules and remain dipic moiety (found  $24.90$ , calcd.  $25.60\%$ ). The exothermic peaks of **2** ( $\text{DTG}_{\text{max}} = 423.8\text{ }^\circ\text{C}$ ) between  $314$  and  $488\text{ }^\circ\text{C}$  correspond to the loss of the three-mole decarboxylate of dipic molecules and remain dipic moiety (found  $35.20$ , calcd.  $36.76\%$ ). The final decomposition products for **1** and **2**, CoO and NiO, were identified by IR spectroscopy (found  $7.50\%$ , calcd.  $9.48\%$ ; found  $8.40\%$ , calcd.  $9.46\%$ ), respectively.

### 3.4. Crystal structure of $(8\text{-H}_2\text{Q})_2[\text{Co}(\text{dipic})_2]\cdot 6\text{H}_2\text{O}$ (**1**) and $(8\text{-H}_2\text{Q})_2[\text{Ni}(\text{dipic})_2]\cdot 6\text{H}_2\text{O}$ (**2**)

The compounds **1** and **2** are isomorphous and crystallize in the monoclinic crystal system space group  $\text{C2/c}$ . Details of crystal structures are given in Table 1. The selected bond distances and angles together with the hydrogen bonding geometry for **1** and **2** are

listed in Tables S4 and S5. The crystallographic analyses revealed that the complexes  $(8\text{-H}_2\text{Q})_2[\text{M}(\text{dipic})_2]\cdot 6\text{H}_2\text{O}$  ( $\text{M} = \text{Co}(\text{II})$  and  $\text{Ni}(\text{II})$ ) consist of a discrete  $[\text{M}(\text{dipic})_2]^{2-}$  anion, two protonated 8-hydroxyquinoline cations, 8- $\text{H}_2\text{Q}$  and six crystal water molecules (Figs. 3 and 4). The M(II) ions has a distorted octahedral geometry with two tridentate dipicolinate ligands. The bisdeprotonated 2,6-pyridinedicarboxylate is coordinated to the M(II) by both the pyridine nitrogen atom and the oxygen atoms of carboxylate groups, creating two chelate ring. The  $\text{M1-N}_{\text{dipic}}$  bond distances are  $2.010(1)$  and  $1.958(1)\text{ \AA}$  in **1** and **2**, respectively, and they are shorter than the  $\text{M-O}_{\text{dipic}}$  bond distances ( $\text{Co1-O1} = 2.155(1)$ ,  $\text{Co1-O3} = 2.168(1)$ ,  $\text{Ni-O1} = 2.121(1)$  and  $\text{Ni-O3} = 2.146(1)\text{ \AA}$ ). The M–N1 and M–O1/O3 bond distances are in agreement with the corresponding values in the related structures  $[\text{Co}(\text{H}_2\text{dipic})(\text{dipic})]\cdot 3\text{H}_2\text{O}$  [ $\text{Co1-O} = 2.108(2)$  and  $2.195(2)\text{ \AA}$ ,  $\text{Co1-N} = 2.017(3)\text{ \AA}$ ] [24],  $[\text{Ni}(\text{H}_2\text{O})_6][\text{Ni}(\text{dipic})_2]\cdot 5\text{H}_2\text{O}$  [ $\text{Ni1-O} = 2.114(2)$ ,  $2.117(2)$ ,  $2.126(2)$  and  $2.147(2)\text{ \AA}$ ,  $\text{Ni1-N} = 1.964(3)$  and  $1.967(3)\text{ \AA}$ ] [32],  $[\text{Ni}(\text{H}_2\text{O})_2(\text{data})_2][\text{Ni}(\text{dipic})_2]\cdot 5\text{H}_2\text{O}$  [ $\text{Ni-O} = 2.104(4)$ ,  $2.109(3)$ ,  $2.137(4)$ ,  $2.187(4)$  and  $\text{Ni-N} = 1.952(4)$ ,  $1.961(4)\text{ \AA}$ ] [33],  $[\text{Ni}(\text{cyclam})(\text{H}_2\text{O})_2][\text{Ni}(\text{dipic})_2]\cdot 2.5\text{H}_2\text{O}$  [ $\text{Ni-O} = 2.132(2)$ ,  $2.146(2)$  and  $\text{Ni-N} = 1.955(3)$ ,  $1.931(3)\text{ \AA}$ ] [5] and  $(\text{HQX})_2[\text{Cu}(\text{HDPC})_2]\cdot 6\text{H}_2\text{O}$  [ $\text{Cu-O} = 2.172(1)$ ,  $2.221(2)$  and  $\text{Cu-N} = 1.932(2)\text{ \AA}$ ] [22]. The bond distances and angles of 8- $\text{H}_2\text{Q}$  ions are in agreement with the corresponding values in the related structures [22,34–36]. Comparison of values of the  $\text{M-O}_{\text{dipic}}$  and  $\text{M-N}_{\text{dipic}}$  distances for the similar 2,6-dicarboxylate complexes can be found in Table 2. The angle of  $\text{N1-M-O1}$  [ $76.31(4)$  and  $78.04(5)^\circ$ ] and  $\text{N1-M-O3}$  [ $76.37(4)$  and  $77.75(5)^\circ$ ] is nearly equal.

The carboxyl groups of the 2,6-pyridinedicarboxylate ligands and water molecules are involved in intermolecular hydrogen bonding with the carboxyl group of dipic ligands and crystal water molecules. The 8- $\text{H}_2\text{Q}^+$  ions are involved in intra- ( $\text{N2-H2}\cdots\text{O5}$  and  $\text{O5-H5A}\cdots\text{O8}$ ) and intermolecular ( $\text{N2-H2}\cdots\text{O4}^{\text{ii}}$ ,  $(\text{ii}) = x + 1/2, y - 1/2, z$ ) hydrogen bonding with the nitrogen atom of pyridine ring, hydroxyl oxygen and water molecule. There are also intramolecular hydrogen bonds  $\text{O5-H5A}\cdots\text{O8}$ ,  $\text{O6-H6A}\cdots\text{O3}$  and  $\text{O7-H7A}\cdots\text{O2}$ . Some of these interactions are illustrated in Fig. 3. There are also  $\text{C-O}\cdots\pi$  interactions between the oxygen atoms ( $\text{C1-O2}$  and  $\text{C7-O4}$ ) of carboxyl group and rings of dipic ligands ( $\text{Cg1} = \text{N}(2)\text{-C}(8)\text{-C}(9)\text{-C}(10)\text{-C}(11)\text{-C}(16)$ ) and  $\text{Cg2} = \text{C}(11)\text{-C}(12)\text{-C}(13)\text{-C}(14)\text{-C}(15)\text{-C}(16)$ ) [the contact distances:  $\text{C1-O2}\cdots\text{Cg1}^{\text{i}} = 3.325$  for **1**,  $3.926\text{ \AA}$  for **2** ( $\text{i} = -1/2 + x, 1/2 - y, 1/2 + z$ ),  $\text{C1-O2}\cdots\text{Cg2}^{\text{ii}} = 3.950$  for **1**,  $3.926\text{ \AA}$  for **2** ( $\text{ii} = 1/2 - x, 1/2 + y, 1/2 - z$ ) and  $\text{C7-O4}\cdots\text{Cg2}^{\text{iii}} = 3.968$  for **1**,  $3.994\text{ \AA}$  for **2** ( $\text{iii} = 1/2 - x, -1/2 + y, 1/2 - z$ ). All of these intermolecular interactions give three-dimensional network results (Tables S4 and S5, Fig. 5).

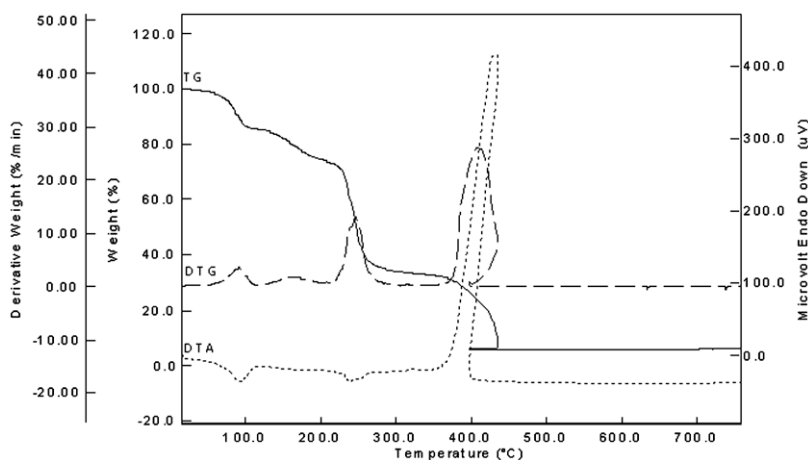


Fig. 1. TG, DTG and DTA curves of (**1**).

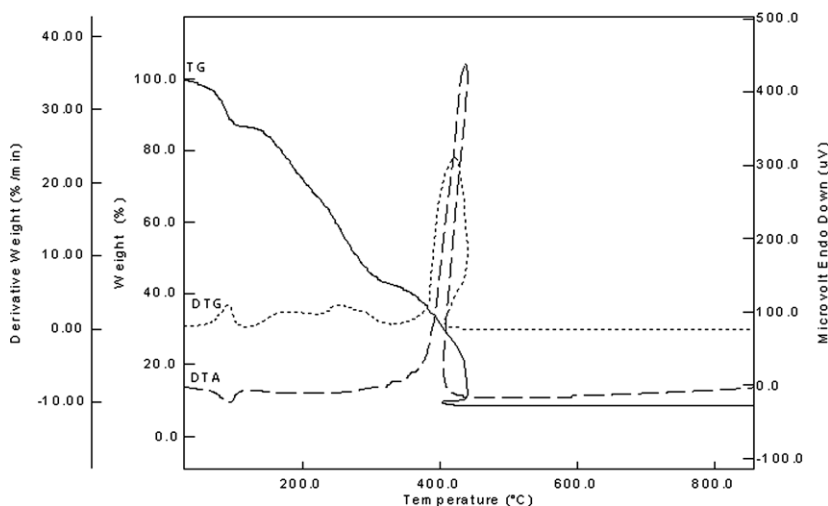


Fig. 2. TG, DTG and DTA curves of (2).

Table 1

Crystal data and structure refinement parameters for the complexes.

	1	2
Empirical formula	C <sub>32</sub> H <sub>34</sub> N <sub>4</sub> O <sub>16</sub> Co	C <sub>32</sub> H <sub>34</sub> N <sub>4</sub> O <sub>16</sub> Ni
Formula weight	789.56	789.34
Temperature (K)	293(2)	293(2)
Wavelength (Å)	0.71073 MoK $\alpha$	
Crystal system	Monoclinic	Monoclinic
Space group	C2/c	C2/c
a (Å)	18.355(1)	18.370(1)
b (Å)	10.3518(4)	10.3476(6)
c (Å)	19.136(1)	19.1539(9)
$\alpha$ , $\beta$ , $\delta$ (°)	90; 110.368(4); 90	90; 111.000(4); 90
V (Å <sup>3</sup> )	3408.7(3)	3399.0(3)
Z	4	4
Absorption coefficient (mm <sup>-1</sup> )	0.59	0.65
D <sub>calc</sub> (mg m <sup>-3</sup> )	1.539	1.542
Theta range for data collection (°)	2.24–27.97	2.24–27.98
Measured reflections	26829	23537
Independent reflections	3343	3332
Absorption correction	Integration Stoe X-RED (Stoe & Cie, 2001)	
Refinement method	Full-matrix least-squares on F <sup>2</sup>	
Final R indices [I > 2 $\sigma$ (I)]	R <sub>int</sub> = 0.047	R <sub>int</sub> = 0.038
Final R indices (all data)	R <sub>1</sub> = 0.030; wR <sub>2</sub> = 0.079	R <sub>1</sub> = 0.030; wR <sub>2</sub> = 0.081
Goodness-of-fit on F <sup>2</sup>	1.04	1.05
$\Delta\rho_{\max}$ (e Å <sup>-3</sup> )	0.19	0.16
$\Delta\rho_{\min}$ (e Å <sup>-3</sup> )	-0.35	-0.35

### 3.5. Cyclic voltammetric studies

Cyclic voltammograms of the Co(II) and Ni(II) metal complexes were run in DMF-0.1M NBu<sub>4</sub>BF<sub>4</sub> as supporting electrolyte at room temperature. Unless otherwise stated, all potentials quoted refer to measurements run at scan rates of 100 and 250 mVs<sup>-1</sup> and against an internal ferrocene–ferrocenium standard. In order to study the effect of the different concentrations of the metal complexes, the electrochemical properties were investigated using the solutions 1.0 × 10<sup>-3</sup> and 1.0 × 10<sup>-4</sup> M and only metal centered. Data obtained from the electrochemical studies were given in Table S6. The electrochemical curves of the Co(II) metal complex at scan rates of 100 and 250 mVs<sup>-1</sup> (1.0 × 10<sup>-3</sup> M) are shown in Figs. 6 and 7. The cv curves of the Co(II) complex at different scan rates and concentrations in dmf solution show the irreversible process ( $I_{pc}$ :  $I_{pa} \neq 1.0$ ). But, the cobalt(II) complex (1.0 × 10<sup>-3</sup> M) shows only reversible process at 0.03 V ( $I_{pc}$ :  $I_{pa} = 1.0$ ) at 250 mVs<sup>-1</sup> scan

rate. At scan rate of 100 mVs<sup>-1</sup> (1.0 × 10<sup>-3</sup> M), its potential range changes from -0.03 to -0.57 V ( $E_{pc}$ ) and -0.74 to 0.03 V ( $E_{pa}$ ). In other words, at scan rates of 100 and 250 mVs<sup>-1</sup> (concentration: 1.0 × 10<sup>-4</sup> M), the anodic and cathodic peak potentials shifted to the more positive regions.

The electrochemical curves of the nickel(II) complex at 100 and 250 mVs<sup>-1</sup> scan rates (1.0 × 10<sup>-3</sup> M) are shown in Figs. S7 and S8. As may be seen from Figs. S7 and S8 and data obtained from Table S6, the reduction–oxidation process of the nickel(II) complex is irreversible. While the cathodic peak potential (0.08 V) at 100 mVs<sup>-1</sup> scan rate (1.0 × 10<sup>-3</sup> M) shifts to more positive region (0.11 V) at 250 mVs<sup>-1</sup> scan rate, the anodic peak potential shifted to the more negative potentials at the same scan rates. Similar results were also obtained when 1.0 × 10<sup>-4</sup> M solution was utilized in dmf. For the cobalt(II) and nickel(II) complexes, although the forward peaks in reduction process in dmf solution and reverse peaks in oxidation process in dmf solution are almost invariant,

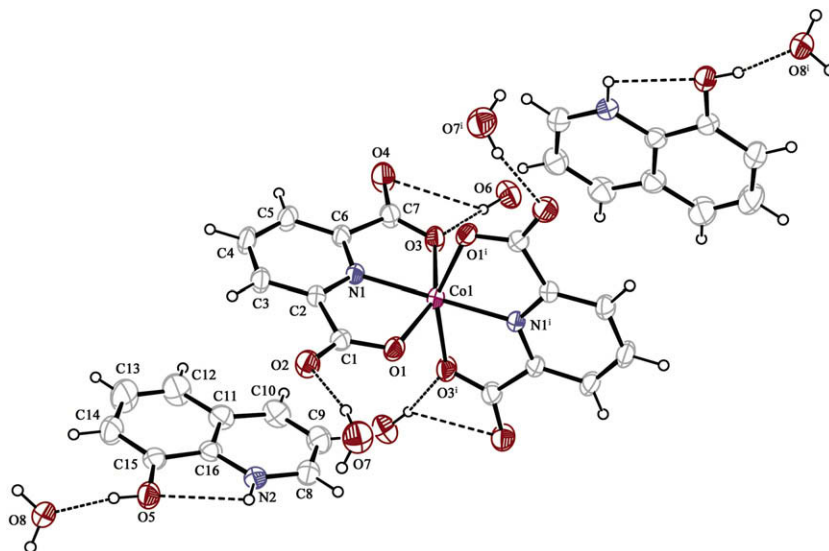


**Fig. 3.** The molecular structure of  $(8\text{-H}_2\text{Q})_2[\text{Co}(\text{dipic})_2]\cdot 6\text{H}_2\text{O}$  (**1**) showing the atom numbering scheme. The thermal ellipsoids are plotted at the 30% probability level ( $i = -x + 1, y, -z + 3/2$ ).

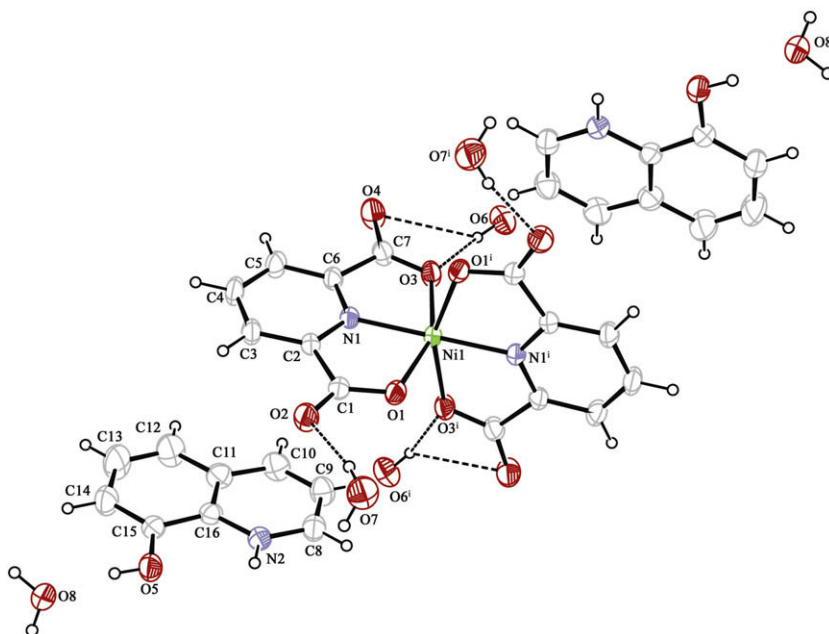


**Fig. 4.** The molecular structure of  $(8\text{-H}_2\text{Q})_2[\text{Ni}(\text{dipic})_2]\cdot 6\text{H}_2\text{O}$  (**2**) showing the atom numbering scheme. The thermal ellipsoids are plotted at the 30% probability level.

**Table 2**  
Comparison of the bond distances (Å) and angles (°) of the pyridine-2,6-dicarboxylic acid complexes.

Complexes	M–O	M–O	M–N	O–M–N	O–M–O
$[\text{Ni}(\text{cyclam})(\text{H}_2\text{O})_2][\text{Ni}(\text{dipic})_2]\cdot 2.5\text{H}_2\text{O}$ , [5]	2.132(2)	2.146(2)	1.931(3)	78.35(5), 78.29(5)	156.70(10)
$[\text{Co}(\text{H}_2\text{dipic})(\text{dipic})]\cdot 3\text{H}_2\text{O}$ , [12]	2.108(2)	2.195(2)	2.017(3)	77.2(1), 75.7(1)	152.9(1)
$\text{Cu}(\text{dipic})(\text{H}_2\text{O})_2$ , [17]	2.002(2)	2.006(2)	1.905(2)	80.70(7), 80.15(7)	160.42(6)
$(\text{HQX})_2[\text{Cu}(\text{Hdipic})_2]\cdot 6\text{H}_2\text{O}$ , [22]	2.172(15)	2.221(16)	1.932(16)	78.25(6), 77.65(6)	155.86(5)
$[\text{Ni}(\text{H}_2\text{O})_6][\text{Ni}(\text{dipic})_2]\cdot 5\text{H}_2\text{O}$ , [32]	2.147(2)	2.126(2)	1.964(3)	77.53(10)	155.68(9)
$[\text{Zn}(\text{H}_2\text{O})_6][\text{Ni}(\text{dipic})_2]\cdot 3\text{H}_2\text{O}$ , [32]	2.115(2)	2.115(2)	1.960(3)	78.09(6)	156.17(8)
$[\text{Ni}(\text{H}_2\text{O})_5\text{Ni}(\text{dipic})_2]\cdot 2\text{H}_2\text{O}$ , [44]	2.164(3)	2.179(3)	1.974(3)	76.97(12), 77.64(12)	154.38(11)
$[\text{Ni}(\text{dipic})(\text{H}_2\text{O})_2]$ , [45]	2.005	2.006	1.903	80.20, 80.41	160.15
$[\text{Ni}(\text{dipic})(\text{bta})_3]$ , [46]	2.586	2.112	1.992	78.39, 76.44	154.82
$[\text{Ni}(\text{dipic})(\text{phen})(\text{H}_2\text{O})]\cdot \text{H}_2\text{O}$ , [47]	2.107(2)	2.132(2)	1.986(2)	78.17, 77.34	155.31(6)
$[\text{Ni}(\text{H}_2\text{dipic})(\text{H}_2\text{O})_3][\text{Ce}(\text{dipic})_3]\cdot 3\text{H}_2\text{O}$ , [48]	2.178(3)	2.172(3)	1.994(3)	76.35(12), 77.11(12)	153.40(11)
$\text{PpzH}_2[\text{Co}(\text{H}_2\text{O})_6][\text{Co}(\text{dipic})_2]\cdot 8\text{H}_2\text{O}$ , [49]	2.153(2), 2.122(2)	2.162(2), 2.193(2)	2.010(2), 2.020(2)	76.50(6), 76.73(6), 75.79(6), 76.99(6)	151.30(6), 152.52(6)
$(8\text{-H}_2\text{Q})_2[\text{Co}(\text{dipic})_2]\cdot 6\text{H}_2\text{O}$ , This work	2.155(1)	2.168(1)	2.010(1)	76.31(4), 76.37(4)	152.61(4)
$(8\text{-H}_2\text{Q})_2[\text{Ni}(\text{dipic})_2]\cdot 6\text{H}_2\text{O}$ , This work	2.121(1)	2.146(1)	1.958(1)	78.04(5), 77.75(5)	155.79(4)

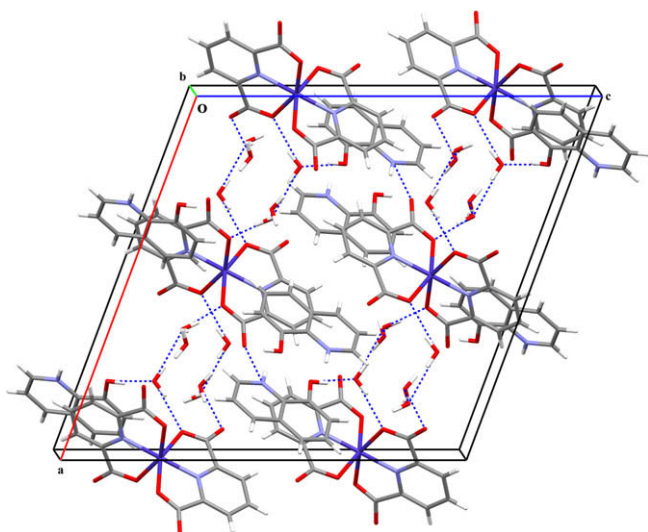


Fig. 5. Packing diagram of (1) viewed along the *a*-axis.

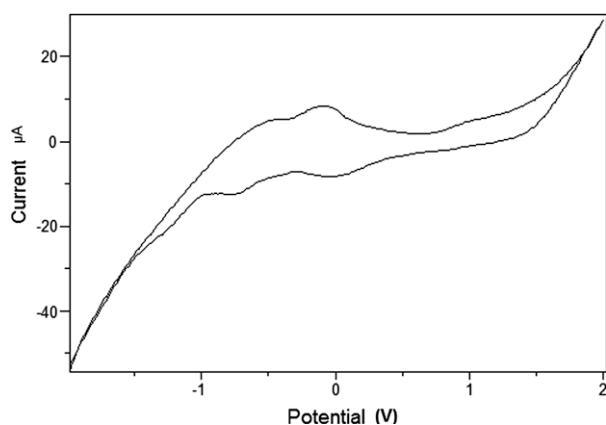


Fig. 6. Cyclic voltammograms of the Co(II) complex in the presence of 0.1 M  $\text{NBu}_4\text{BF}_4$  in DMF (sr:  $100 \text{ mVs}^{-1}$ ,  $1 \times 10^{-3} \text{ M}$ ).

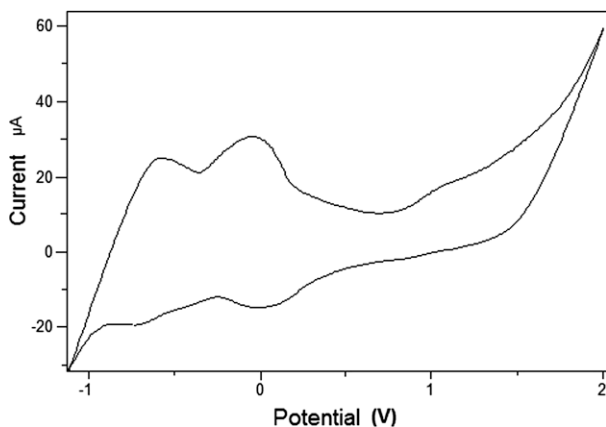


Fig. 7. Cyclic voltammograms of the Co(II) complex in the presence of 0.1 M  $\text{NBu}_4\text{BF}_4$  in DMF (sr:  $250 \text{ mVs}^{-1}$ ,  $1 \times 10^{-3} \text{ M}$ ).

the position and broadness of the return peak varies markedly depending on the anion present. This suggests that close association of the anions with the metal(II) centers may occur following reduction on the electrode surface. No  $\text{M}^{\text{I}}-\text{M}^{\text{O}}$  (M: Co(II) and Ni(II))

reduction was detected for the metal complexes. All of the complexes were sufficiently soluble in dmf to allow a cyclic voltammogram to be run. In dmsolvent, the complexes show an identical pattern of peaks. However, in generally, the potentials of all these processes are slightly more positive in dmsolvent than their positions in dmf.

### 3.6. Antimicrobial activity

In this study, *in vitro* potential antimicrobial activity of  $\text{H}_2\text{dipic}$ , 8-HQ,  $[\text{Co}(\text{H}_2\text{dipic})(\text{dipic})] \cdot 3\text{H}_2\text{O}$  [12], **1**,  $[\text{Ni}(\text{Hdipic})_2] \cdot 3\text{H}_2\text{O}$  [29], **2** were tested according to agar well diffusion method. Table 3 shows the effect of 11 different concentrations against the growth of Gram-positive, Gram-negative bacterial strains, yeast strain and fungal strain. We look into compound **1** which displayed the inhibitory effect against all tested Gram-positive bacteria (*S. aureus*, *B. subtilis*) and yeast and mold (*C. albicans*, *A. niger*) except Gram-negative bacteria (*E. coli*, *S. typhimurium*). Inhibitory effect against Gram-positive bacteria and yeast and mold was observed in compound **2**. The main reason for the antimicrobial activity in compounds **1** and **2** are related to presence of 8-HQ. In light of these results, it appears that, compound **1** and **2** showed same antimicrobial activity against tested microorganisms. In classifying the antibacterial activity as Gram-positive or Gram-negative, it would generally be expected that a much greater number would be active against Gram-positive than Gram-negative bacteria [37]. The outer membrane of Gram-negative bacteria is the first barrier capable of limiting the penetration of antimicrobial agents. This fact is widely known and referred to as “intrinsic resistance” of Gram-negative bacteria [38]. Our study results had showed also the same effect.

As can be seen from Table 3,  $[\text{Co}(\text{H}_2\text{dipic})(\text{dipic})] \cdot 3\text{H}_2\text{O}$  did not show any antimicrobial activity against tested microorganisms at applied concentrations. Pyridine-2,6-dicarboxylic acid did not show antimicrobial activity against *E. coli*, *S. typhimurium* but weak antimicrobial activity against *B. subtilis* and *C. albicans* and *A. niger*. 8-HQ showed good inhibitory effect against tested total microorganisms  $[\text{Ni}(\text{Hdipic})_2] \cdot 3\text{H}_2\text{O}$  showed weak or absent antimicrobial activity at  $250 \mu\text{g}/\text{well}$ . It is interesting that complexation protects the microorganisms, again consistent with the free ligand being more potent than the complex. While inert Mo compounds are the least effective at inhibiting yeast growth, Mo-dimethylhydroxylamido complex is the most effective [39]. These results show that the formation of some Mo complexes can protect yeast from the growth inhibition observed when either the ligand or Mo salt alone is present [39]. But this effect was not observed for the vanadium insulin-enhancing compounds [10–11]. These studies have revealed many compounds which exhibited good antimicrobial effect  $(8\text{-H}_2\text{Q})_2[\text{Mn}(\text{dipic})_2(\text{dipic})] \cdot 6\text{H}_2\text{O}$  and  $(8\text{-H}_2\text{Q})_2[\text{Zn}(\text{dipic})_2(\text{dipic})] \cdot 6\text{H}_2\text{O}$  showed good inhibition effect against Gram-positive bacteria and fungi. No growth inhibition was observed against tested Gram-negative bacteria [40]. The activity of the new synthesis complexes increases as the concentration increases because concentration is well known to play a vital role in increasing the degree of inhibition [13]. In a previous study, Co(III) complexes of pyridine-2,6-dicarboxylic acid, pyridine-2,5-dicarboxylic acid, pyridine-3,5-dicarboxylic acid, and pyridine-3,4-dicarboxylic acid were synthesized and characterized using the “Field-Durant Green” solution as starting material  $(\text{K}_3[\text{Co}(\text{III})(\text{CO}_3)_3])$ . The mutagenic activity of the  $\text{K}[\text{Co}(\text{III})(\text{dipic})_2]$  ( $\text{H}_2\text{dipic}$  = pyridine-2,6-dicarboxylic acid) complex was tested according to Ames [41,42] with *S. typhimurium* TA 98 and TA 100 strains. Tests carried out on the complex proved it to be a non-mutagenic compound [14].

A pyrazolate bridged binuclear Pd(II) complex  $[\text{Pd}_2(\mu\text{-dppz})_2(\text{Hida})_2] \cdot \text{CH}_3\text{OH} \cdot 2\text{H}_2\text{O}$  ( $\text{dppz}$  = 3,5-diphenylpyrazolate) with monoprotonated iminodiacetate (Hida) and a mononuclear Pt(II) complex containing Hdppz and 2,6-pyridinedicarboxylate

**Table 3**Antibacterial and antifungal activity [Co(H<sub>2</sub>dipic)(dipic)]·3H<sub>2</sub>O [29], 8-HQ, **1**, [Ni(Hdipic)<sub>2</sub>]·3H<sub>2</sub>O [30], **2** as inhibition zones (mm) (well Ø10 mm).

Compound	Strains	Concentrations (µg/well)									
		250	125	62.5	31.2	15.6	7.8	3.9	1.9	0.9	0.4
8-HQ	<i>B. subtilis</i>	53 ± 0.4	48 ± 0.7	32 ± 0.8	26 ± 1.1	19 ± 1.2	12 ± 1.3	–	–	–	–
	<i>S. aureus</i>	68 ± 0.7	54 ± 0.9	41 ± 0.7	30 ± 0.5	22 ± 0.7	16 ± 0.7	13 ± 1.1	11 ± 0.4	–	–
	<i>E. coli</i>	32 ± 0.7	28 ± 1.2	22 ± 1.9	17 ± 1.2	12 ± 1.6	–	–	–	–	–
	<i>S. typhimurium</i>	25 ± 1.4	20 ± 1.6	18 ± 1.2	14 ± 1.4	–	–	–	–	–	–
	<i>C. albicans</i>	54 ± 0.7	50 ± 1.2	31 ± 1.3	20 ± 1.5	15 ± 1.3	–	–	–	–	–
	<i>A. niger</i>	56 ± 0.8	51 ± 1.5	48 ± 1.2	40 ± 1.4	31 ± 0.6	22 ± 1.6	14 ± 1.3	–	–	–
H <sub>2</sub> dipic	<i>B. subtilis</i>	18 ± 0.4	16 ± 0.4	15 ± 0.6	14 ± 0.1	13 ± 0.5	12 ± 0.8	–	–	–	–
	<i>S. aureus</i>	12 ± 0.4	–	–	–	–	–	–	–	–	–
	<i>E. coli</i>	–	–	–	–	–	–	–	–	–	–
	<i>S. typhimurium</i>	–	–	–	–	–	–	–	–	–	–
	<i>C. albicans</i>	15 ± 0.4	14 ± 0.4	13 ± 0.6	12 ± 0.1	–	–	–	–	–	–
	<i>A. niger</i>	14 ± 0.4	12 ± 0.4	–	–	–	–	–	–	–	–
[Co(H <sub>2</sub> dipic)(dipic)]·3H <sub>2</sub> O, [29]	<i>B. subtilis</i>	–	–	–	–	–	–	–	–	–	–
	<i>S. aureus</i>	–	–	–	–	–	–	–	–	–	–
	<i>E. coli</i>	–	–	–	–	–	–	–	–	–	–
	<i>S. typhimurium</i>	–	–	–	–	–	–	–	–	–	–
	<i>C. albicans</i>	–	–	–	–	–	–	–	–	–	–
	<i>A. niger</i>	–	–	–	–	–	–	–	–	–	–
<b>1</b>	<i>B. subtilis</i>	28 ± 1.7	25 ± 1.3	21 ± 0.4	18 ± 1.3	15 ± 0.4	12 ± 0.9	–	–	–	–
	<i>S. aureus</i>	38 ± 1.2	29 ± 0.4	20 ± 1.3	15 ± 0.4	12 ± 0.8	–	–	–	–	–
	<i>E. coli</i>	–	–	–	–	–	–	–	–	–	–
	<i>S. typhimurium</i>	–	–	–	–	–	–	–	–	–	–
	<i>C. albicans</i>	26 ± 1.1	18 ± 0.8	15 ± 0.4	12 ± 0.2	–	–	–	–	–	–
	<i>A. niger</i>	51 ± 0.4	48 ± 0.9	38 ± 0.3	24 ± 0.4	18 ± 0.4	14 ± 0.8	–	–	–	–
[Ni(Hdipic) <sub>2</sub> ]·3H <sub>2</sub> O, [30]	<i>B. subtilis</i>	11 ± 0.5	–	–	–	–	–	–	–	–	–
	<i>S. aureus</i>	–	–	–	–	–	–	–	–	–	–
	<i>E. coli</i>	–	–	–	–	–	–	–	–	–	–
	<i>S. typhimurium</i>	–	–	–	–	–	–	–	–	–	–
	<i>C. albicans</i>	11 ± 0.1	–	–	–	–	–	–	–	–	–
	<i>A. niger</i>	12 ± 0.8	–	–	–	–	–	–	–	–	–

–, no inhibition of zone. All the microorganisms were resistant to the control DMSO.

(dipic)[Pt(Hdppz)(dipic)]·CH<sub>3</sub>OH are synthesized. Moderate luminescence property and antimicrobial activity against *B. subtilis* have been noted for both [16].

Mononuclear complexes M(L)Cl<sub>2</sub> where M = Mn(II), Fe(II), Co(II), Ni(II) and Cu(II) and (L = N,N-diethylpiperaziny1,2,6-pyridinedicarboxylate) have been synthesized. Antimicrobial activities of newly synthesized complexes were investigated against some Gram-positive and Gram-negative bacteria such as, *E. coli*, *S. aureus*, *C. albicans* and *A. flavus*. The activity of Mn(II), Fe(II) and Co(II) complexes have been observed as lower than that of Cu(II) complex [15]. The antimicrobial activity of the metal complexes generally depend on the following factors: the chelation ability of the ligand, the nature of nitrogen donor ligands, the total charge of the complex, the existence and the nature of the metal ion neutralizing the ionic complex and the nuclearity of the metal center in the complex [43].

#### 4. Conclusion

In summary, two new compounds (8-H<sub>2</sub>Q)<sub>2</sub>[M(dipic)<sub>2</sub>]·6H<sub>2</sub>O (M = Co (**1**) and Ni (**2**), 8-HQ = 8-hydroxyquinoline, dipic = dipicolinate) have been prepared and characterized by elemental analysis, spectral (IR and UV–vis), thermal analyses, magnetic measurements and single-crystal X-ray diffraction techniques. The compounds **1** and **2** are isomorphous and crystallize in the monoclinic crystal system space group C2/c. The common bond distances and angles of (**1**) and (**2**) are in agreement with the corresponding values in the literature structures. As for bond distances, M–O and M–N of (**1**) and (**2**) have showed significant changes according to precursors. The M(II) ions has a distorted octahedral geometry with two tridentate dipicolinate ligands.

Strong hydrogen bonds between uncoordinated water, (8-H<sub>2</sub>Q)<sup>+</sup> and carboxylate play important roles in the construction of the supramolecular networks. The decrease in biological activity of ligands has also been observed in complex **1** and **2** which has previously been experienced in molybdenum complexes due to complexation.

#### Acknowledgments

The authors are indebted to the Dumluşinar University Research Found for support (Grant No: 2007/14). The authors would like to thank to Prof. Dr. Mehmet Tümer (University of Kahramanmaraş Sütçü İmam) for assistance in cyclic voltammetric studies of **1** and **2**.

#### Appendix A. Supplementary data

Crystallographic data for the structure reported here have been deposited at the CCDC as supplementary data, CCDC No. 675198 and 675199. Copies of the data available at CCDC, 12 Union Road, Cambridge CB2 1EZ, UK. E-mail: deposit@ccdc.cam.ac.uk. Materials and equipment of cyclic voltammograms, Tables S3–S6 of bond angles and hydrogen bond geometries of complexes, CV graphic of **2** and electronic absorption spectra of **1** and **2** as well as their precursors are also available. Supplementary data associated with this article can be found, in the online version, at doi:10.1016/j.molstruc.2009.07.026.

## References

- [1] J.R.H. Xie, V.H. Smith Jr., R.E. Allen, *Chem. Phys.* 322 (2006) 254.
- [2] M.V. Kirillova, M.F.C.G. Da Silva, A.M. Kirillov, J.J.R.F. Da Silva, A.J.L. Pombeiro, *Inorg. Chim. Acta* 360 (2007) 506.
- [3] Z. Vargova, V. Zeleoaq, I. Cisaova, K. Györyova, *Thermochim. Acta* 423 (2004) 149.
- [4] D.C. Crans, A.M. Trujillo, S. Bonetti, C.D. Rithner, B. Baruah, N.E. Levinger, *J. Org. Chem.* 73 (2008) 9633.
- [5] H. Park, A.J. Lough, J.C. Kim, M.H. Jeong, Y.S. Kang, *Inorg. Chim. Acta* 360 (2007) 2819.
- [6] A. Szorcik, L. Nagy, A. Deak, M. Scopelliti, Z.A. Fekete, A. Csaszar, C. Pellerito, L. Pellerito, *J. Organo. Chem.* 689 (2004) 2762.
- [7] İ. Uçar, B. Karabulut, A. Bulut, O. Büyükgüngör, *J. Mol. Struct.* 834–836 (2007) 336.
- [8] A. Moghimi, S.M. Moosavi, D. Kordestani, B. Maddah, M. Shamsipur, H. Aghabozorg, F. Ramezanipour, G. KICKELBICK, *J. Mol. Struct.* 828 (2007) 38.
- [9] D.C. Crans, *J. Inorg. Biochem.* 80 (2000) 123.
- [10] D.C. Crans, J.J. Smee, E. Gaidamauskas, L. Yang, *Chem. Rev.* 104 (2004) 849.
- [11] P. Buglyo, D.C. Crans, E.M. Nagy, R.L. Lindo, L. Yang, J.J. Smee, W. Jin, L.H. Chi, M.E. Godzala, G.R. Willsky, *Inorg. Chem.* 44 (2005) 5416.
- [12] L. Yang, D.C. Crans, S.M. Miller, A. Cour, O.P. Anderson, P.M. Kaszynski, M.E. Godzala, L.T.D. Austin, G.R. Willsky, *Inorg. Chem.* 41 (2002) 4859.
- [13] A.A. El-Sherif, B.J.A. Jeragh, *Spectrochim. Acta A* 68 (2007) 877.
- [14] A.Y.A. Mohamed, S.A.W. Al-Arrayed, *Synt. React. Inorg. Met. Org. Chem.* 32 (2002) 1759.
- [15] S. Khan, S.A.A. Nami, K.S. Siddiqi, E. Husain, I. Naseem, *Spectrochim. Acta A* 72 (2009) 421.
- [16] J. Chakraborty, M.K. Saha, P. Banerjee, *Inorg. Chem. Commun.* 10 (2007) 671.
- [17] M. Koman, J. Moncol, D. Hudecova, B. Dudova, M. Melnik, M. Korabik, J. Mrozinski, *Polish. J. Chem.* 75 (2001) 957.
- [18] İ. Uçar, A. Bulut, A. Karadağ, C. Kazak, *J. Mol. Struct.* 837 (2007) 38.
- [19] İ. Uçar, A. Bulut, O. Büyükgüngör, *J. Phys. Chem. Sol.* 68 (2007) 2271.
- [20] J.C. Mac Donald, P.C. Dorresteijn, M.M. Pilley, M.M. Foote, J.L. Lundburg, R.W. Henning, A.J. Schultz, J.L. Manson, *J. Am. Chem. Soc.* 122 (2000) 11692.
- [21] H. Aghabozorg, J.A. Gharamaleki, P. Ghasemikhah, M. Ghadermazi, J. Soleimannejad, *Acta Crystallogr.* E63 (2007) m1710.
- [22] Y.M. Jiang, X.J. Yin, *Chin. J. Inorg. Chem.* 17 (2001) 589.
- [23] Z.A. Kaplancıklı, G.T. Zitouni, A. Özdemir, G. Revial, *Eur. J. Med. Chem.* 43 (2008) 155.
- [24] Stoe & Cie X-Area (Version 1.18) and X-Red32 (Version 1.04) (2001) Stoe & Cie, Darmstadt, Germany, 2002.
- [25] G.M. Sheldrick, SHELXS97 and SHELXL97, University of Göttingen, Göttingen, Germany, 1997.
- [26] L.J. Farrugia, *J. Appl. Crystallogr.* 30 (1997) 565.
- [27] K. Güven, E. Yücel, F. Çetintaş, *Pharm. Biol.* 44 (2006) 79.
- [28] National Committee for Clinical Laboratory Standards (NCCLS), Methods for dilution antimicrobial susceptibility tests for bacteria that grow aerobically, Approved Standard (M7-A2), National Committee for Clinical Laboratory Standards, Villanova, PA, 1990, pp. 8.
- [29] L.C. Nathan, T.D. Mai, *J. Chem. Crystallogr.* 30 (2000) 509.
- [30] D.F. Shriver, P.W. Atkins, C.H. Langford, *Inorganic Chemistry*, Oxford University Press, Oxford, 1994, pp. 252.
- [31] K. Nakamoto, *Infrared and Raman Spectra of Inorganic and Coordination Compounds*, fifth ed., Wiley Interscience, New York, 1997, pp. 59.
- [32] M.V. Kirillova, A.M. Kirillov, M.F.C.G. Da Silva, M.N. Kopylovich, J.J.R.F. Da Silva, A.J.L. Pombeiro, *Inorg. Chim. Acta* 361 (2008) 1728.
- [33] L.J. Zhang, B.X. Liu, H.Q. Ge, D.J. Xuc, *Acta Crystallogr.* E62 (2006) m2180.
- [34] G. Smith, U.D. Wermuth, P.C. Healy, *Acta Crystallogr.* C60 (2004) o600.
- [35] G. Smith, U.D. Wermuth, P.C. Healy, J.M. White, *Acta Crystallogr.* E62 (2006) o5089.
- [36] T. Kolev, S.S. Fiser, M. Spitteller, W.S. Sheldrick, H.M. Figge, *Acta Crystallogr.* E61 (2005) o146.
- [37] A.R.M. Cutheon, S.M. Ellis, R.E.W. Hancock, G.H.N. Towers, *J. Ethnopharmacol.* 37 (1992) 213.
- [38] N.V. Loginova, T.V. Kovalchuk, R.A. Zheldakova, N.P. Osipovich, V.L. Sorokin, G.I. Polozov, G.A. Ksedzova, G.K. Glushonak, A.A. Chernyavskaya, O.I. Shadyro, *Bioorg. Med. Chem. Lett.* 16 (2006) 5403.
- [39] D.C. Crans, J.J. Smee, E.G. Gaidamauskiene, O.P. Anderson, S.M. Miller, W. Jin, E. Gaidamauskas, E. Crubellier, R. Grainda, L.H. Chi, G.R. Willsky, *J. Inorg. Biochem.* 98 (2004) 1837.
- [40] A.T. Çolak, F. Çolak, O.Z. Yeşilel, O. Büyükgüngör, *J. Coord. Chem.* 62 (2009) 1650.
- [41] B.N. Ames, J. McCann, E. Yamasaki, *Mutat. Res.* 31 (1975) 347.
- [42] D.M. Maron, B.N. Ames, *Mutat. Res.* 113 (1983) 173.
- [43] G. Psomas, A. Tarushi, E.K. Efthimiadou, Y. Sanakis, C.P. Raptopoulou, N. Katsaros, *J. Inorg. Biochem.* 100 (2006) 1764.
- [44] Y.H. Wen, Z.J. Li, Y.Y. Qin, Y. Kang, Y.B. Chen, J.K. Cheng, Y.G. Yao, *Acta Crystallogr.* E58 (2002) m762.
- [45] Y. Liu, J.M. Dou, D. Wang, X.X. Zhang, L. Zhou, *Acta Crystallogr.* E62 (2006) m2208.
- [46] P. Ramadevi, S. Kumaresan, K.W. Muir, *Acta Crystallogr.* E61 (2005) m1749.
- [47] P. Ramadevi, S. Kumaresan, N. Sharma, *Acta Crystallogr.* E62 (2006) m2957.
- [48] T.K. Prasad, M.V. Rajasekharan, *Polyhedron* 26 (2007) 1364.
- [49] H. Aghabozorg, J.A. Gharamaleki, M. Ghadermazi, P. Ghasemikhah, J. Soleimannejad, *Acta Crystallogr.* E63 (2007) m1803.